Large amplitude motion in "BD_v3_x3p9_y1p5_z40.table / QF_v3_x3p9_y1p5_z40.table" cell

This Note addresses large amplitude properties of the arc cell, using the OPERA 3-D field maps "BD_v3_x3p9_y1p5_z40.table" and "QF_v3_x3p9_y1p5_z40.table" [1].

Accurate properties of FFAG cells can only be determined based on accurate field models - just the same way as magnet and lattice design goes - and that holds for orbits, focusing and higher order parameters including chromaticity, amplitude detuning, dynamical admittance and other feed down [2]. For this reason the OPERA 3-D field map of the QF and BD magnets are used. Note that using field maps requires stepwise integration of the equation of motion, which is the method retained in producing the beam dynamics results discussed here.

Due the cell magnets being short, as was the case in the earlier, similar, EMMA FFAG cell [3], the field along the orbits does not feature any plateau (Fig. 2). As a consequence it has a rich content in derivatives (Fig. 3), as can be inferred from the scalar potential from which it derives, namely, $B_s = \partial V/\partial s$, $B_x = \partial V/\partial x$, $B_y = \partial V/\partial y$, with

$$V_1(s,x,y) = G_1(s)y - \frac{G_1^{(2)}(s)}{8}(x^2+y^2)y + \frac{G_1^{(4)}(s)}{192}(x^2+y^2)^2y + ... \quad \text{(dipole)}$$

$$V_2(s,x,y) = G_2(s)xy - \frac{G_2^{(2)}(s)}{12}(x^2+y^2)xy + \frac{G_2^{(4)}(s)}{384}(x^2+y^2)^2xy + ... \quad \text{(quadrupole)}$$

In these expressions, s, x, y are respectively the longitudinal, transverse-horizontal and -vertical coordinates in the magnets with the latter two taken from the multipole axis, and $G_{1,2}(s)$ is the longitudinal form factor and $G_{1,2}^{(n)} = d^nG_{1,2}/ds^n$. Note that non-zero vertical motion introduces non-linear coupling.

An ideal cell without any random errors (neither field not alignment) is considered. Yet it does include systematic non-linearities, namely, (i) the multipole content intrinsic to the magnet geometry in the OPERA simulation, and (ii) the non-linearity content resulting from the longitudinal form factor as addressed above. Note that the latter includes all orders in x, y, yet without the multipole symmetries.

Note also : field maps are scaled to 98% field [4].

Properties of the arc cell are summarized in a series of figures, as follows.

◇ A scan of the paraxial conditions of the cell as of stepwise integration, thus including all possible multipole feed downs, is shown in Fig. 1, this establishes the optics working hypotheses, together with Table 1 which details some of the values of concern, and with orbit and field details displayed in Appendix.

◇ Admittances for a 1000-cell beam line, as observed from the center of the long drift, are displayed Fig. 4, for the four design energies and two additional ones to assess viability margins beyond the useful range.

◇ A scan of the admittance value over that extended energy interval 40.5-160 MeV is displayed in Fig. 5, which shows an increase from ≈7 mm at 42 MeV to ≈700 mm at 150 MeV. The result appears to be weakly dependent on the number of cells beyond about 200 cells.

◇ Instances of maximum stable amplitude motion in phase space, *i.e.*, typical samples of the data that lead to the admittances in Figs. 4, 5, are displayed in Fig. 6 and Fig. 7 :

- In the horizontal phase space case, the initial vertical invariant is taken quasi-zero. The island portrait at 42 MeV stems from weak dodecapole non-linearities, while $Q_x = 2/5$ (Fig. 8). Coupling is significant at 78 MeV which spirals out to lager invariant and, outside nominal range, at 160 MeV which goes off-centered (Fig. 6-right).

- In the vertical phase space case, the initial horizontal invariant is taken quasi-zero, however, non-linear coupling causes it to grow significantly at all six energies (Fig. 7-left).

Table 1: Tunes as a function of total energy, paraxial and, in order to give a taste of extremum amplitude detuning (see tune diagrams in Figs. 8, 9, for more), at maximum stable amplitudes, either H (this refers extreme amplitude phase space motion as displayed in Fig. 6) or V (motion in Fig. 7).

Energy/MeV	40	42	78	114	150	160
Paraxial motion						
Q_x	0.431285	0.386643	0.184001	0.126835	0.100490	0.096293
Q_y	0.321481	0.297893	0.129553	0.067649	0.032579	0.026764
At maximum stable H amplitude						
Q_x	0.457136	0.400119	0.189284	0.130336	0.102693	0.097575
Q_y	0.318734	0.299796	0.121668	0.061034	0.02471	0.013564
At maximum stable V amplitude						
Q_x	$0.340245^{(a)}$	0.392520	0.180536	0.127657	0.179010	0.088168
Q_y	$0.329877^{(a)}$	0.301043	0.132415	0.076341	0.055848	0.044013

(a) Typical of non-linear coupling observed at large amplitude, the horizontal motion has more than one line, see Fig. 10

◇ The effect of anharmonicities (*i.e.*, horizontal $dQx/d\epsilon_x$, $dQx/d\epsilon_y$, and vertical $dQy/d\epsilon_x$, $dQy/d\epsilon_y$) are represented in the tune diagrams in Fig. 8 and Fig. 9, via amplitude detuning for about 20 initial invariant values (for each one of the 6 energies considered) ranging evenly from paraxial up to maximum stable amplitude (Figs. 6 and 7). Tunes are computed by discrete Fourier transform, from 400-cell tracking. The two figures show respectively the case of large amplitude horizontal motion (that shown in Fig. 6) and large amplitude vertical motion (Fig. 7).

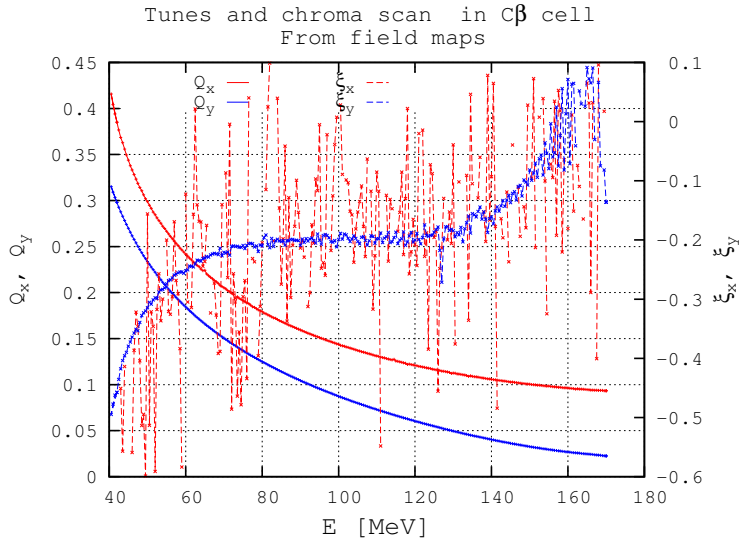

Figure 1: Energy dependence of cell tunes and chromaticities. An energy range extending to 40 MeV to the left and 170 MeV to the right, slightly beyond the {42,78,114,150} MeV set, is considered in order to check periodic stability margins.

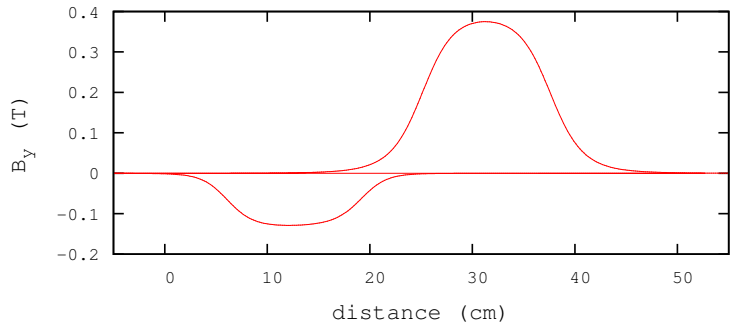

Figure 2: Typical field contributions along an orbit (114 MeV orbit here), from the QF (left bump) and BD (right) magnets. This illustrates the typical shape of the longitudinal form factor G(s) discussed in the text. The field in the numerical integration of particle motion is the sum of these two contributions.

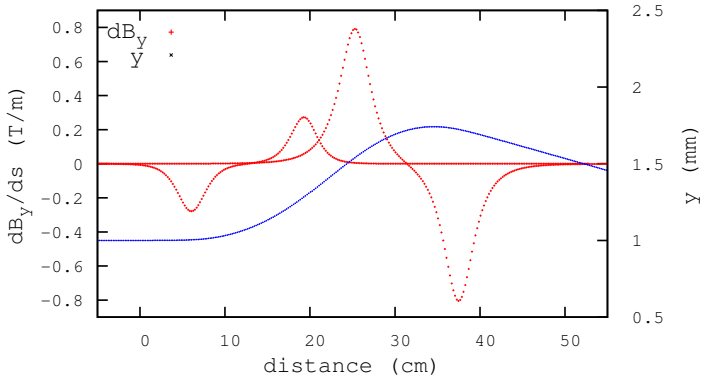

Figure 3: First order derivatives dB_y/ds along QF and BD (red dotted curves) for a 114 MeV trajectory with vertical coordinate represented by the blue curve. The field integrals far from cancel as the vertical coordinate changes drastically across the magnets.

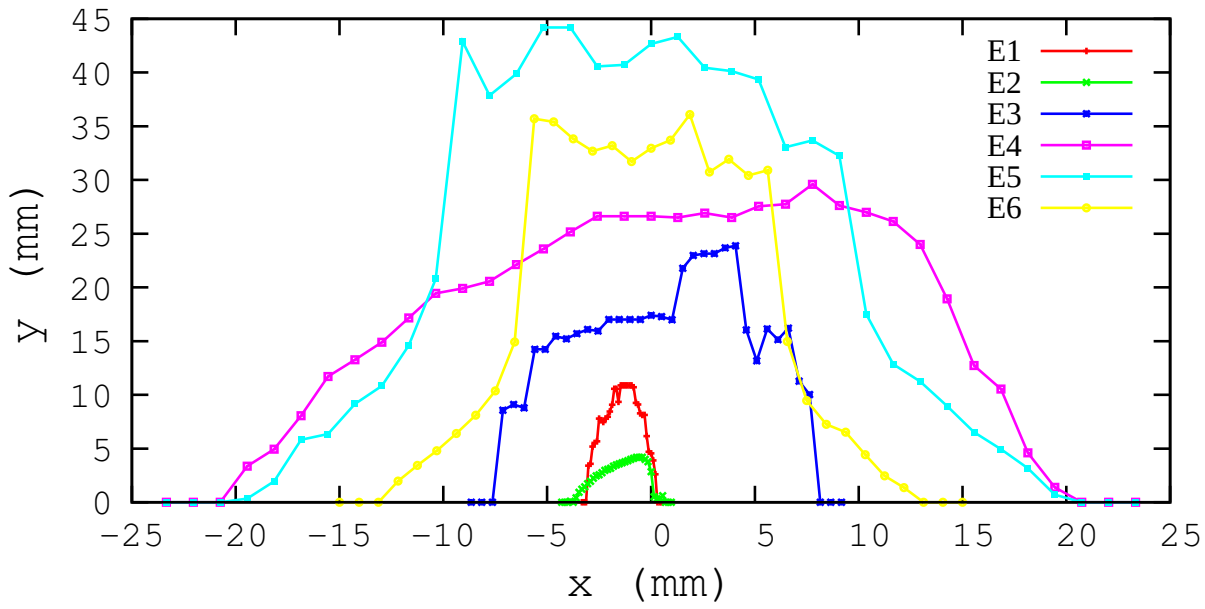

Figure 4: Dynamical admittance of a beam line made up of 1000 CBETA arc cells, at energies E1-6 = 40.5, 42, 78, 114, 150 and 160 MeV.

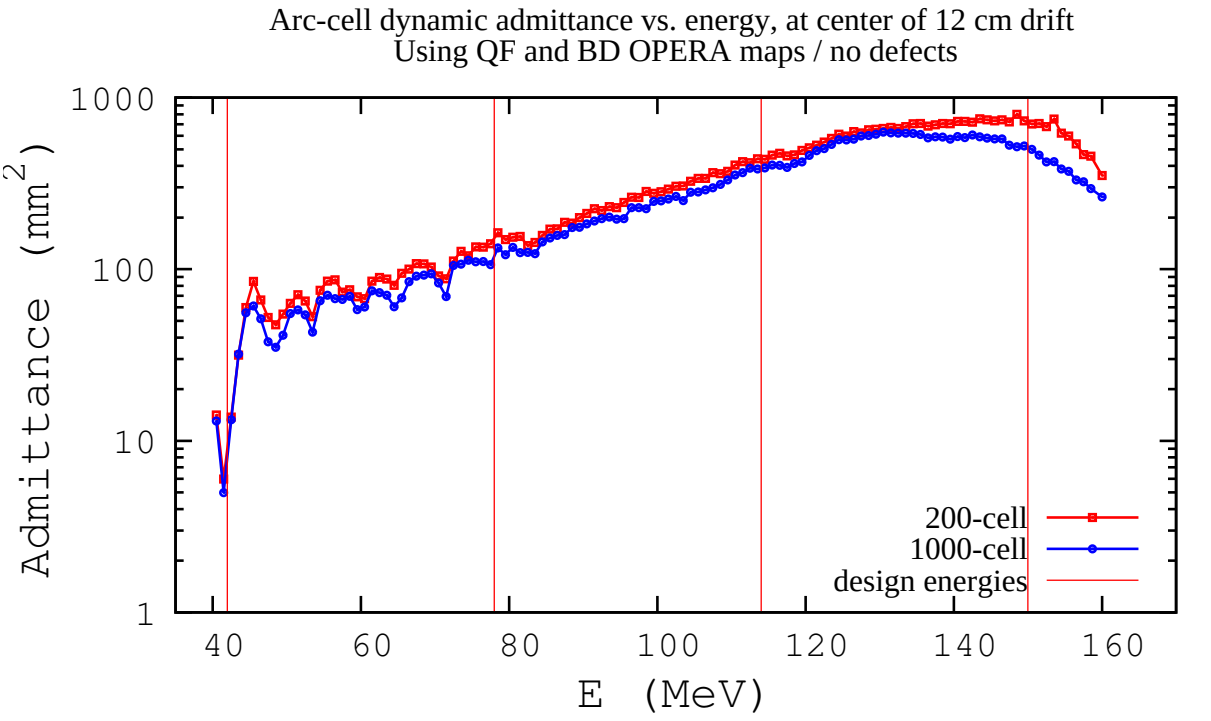

Figure 5: A scan of dynamical admittance value over 40.5-160 MeV, for 200-cell and 1000-cell beam lines. Cell parameters (or energy range ?) need be tweaked to move the low energy pass to the right of the present dip in the 42 MeV region.

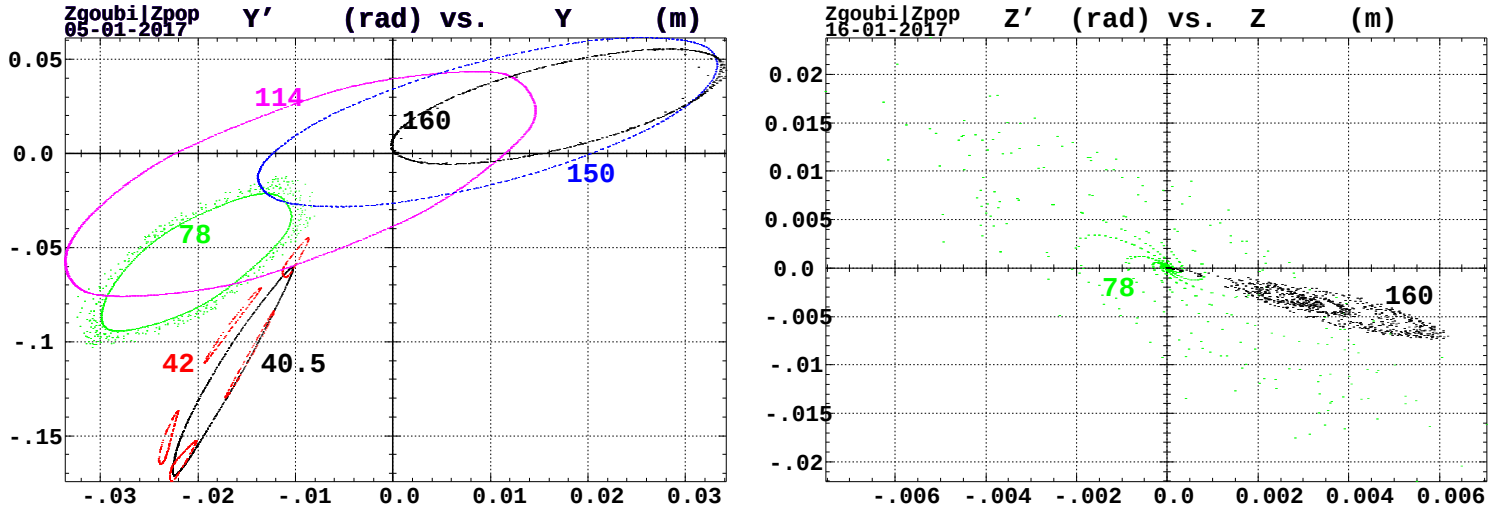

Figure 6: Left : 1000-cell maximum horizontal stable amplitude. Right : corresponding vertical phase-space - 78 MeV and 160 MeV undergo substantial growth, from quasi-zero initial invariant, the other 4 energies maintain their vertical invariant small.

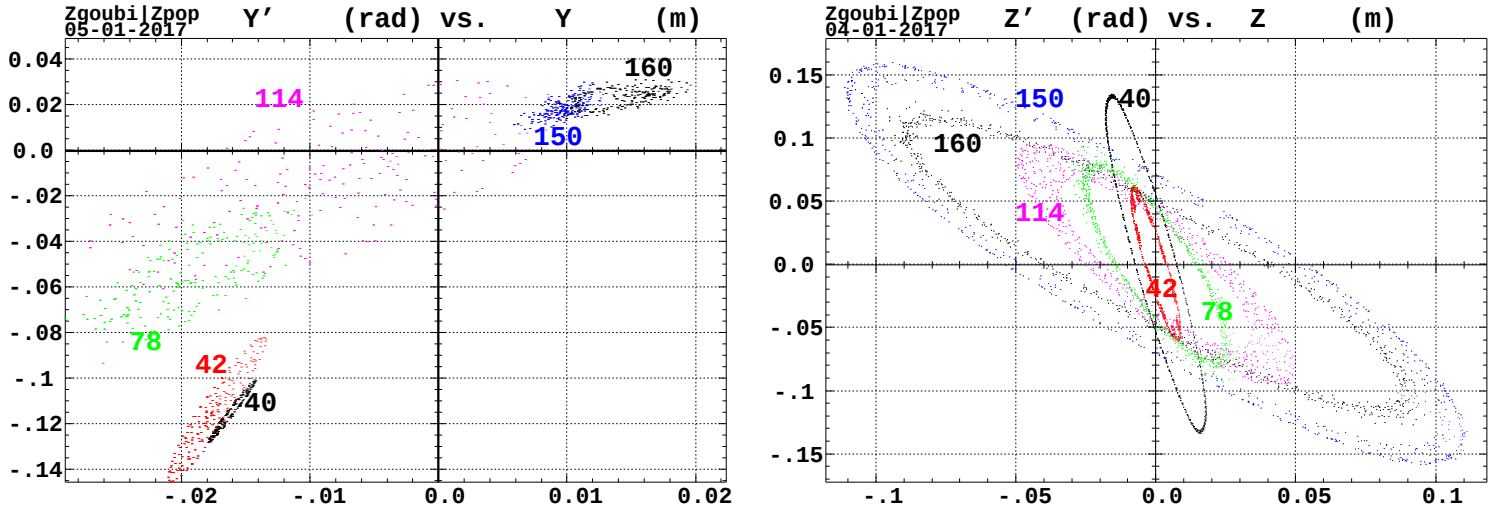

Figure 7: Right : 1000-cell maximum vertical stable amplitude. Left : corresponding horizontal phase-space, for quasi-zero initial horizontal invariant.

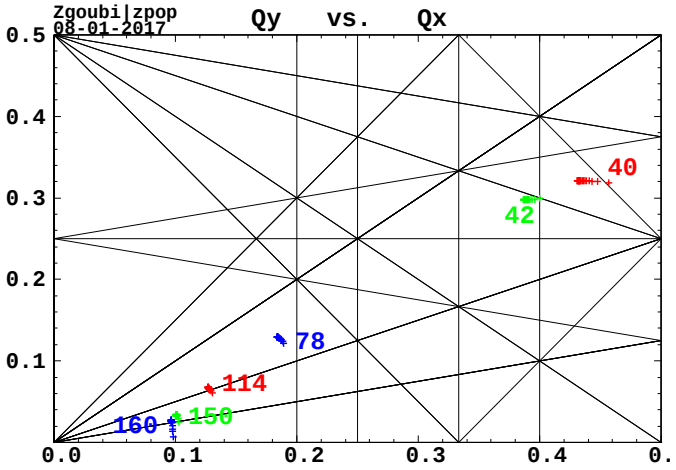

Figure 8: Spreading of $Q_x,\ Q_y$ tunes under the effect of horizontal anharmonicities, up to maximum stable horizontal amplitude. Resonance lines $mQ_x + nQ_Y$ =integer are for upright multipoles, up to $|m| + |n| = 5$. For each energy a few tune values are plotted, corresponding to particles launched with initial horizontal invariants evenly distributed from paraxial to maximum amplitude.

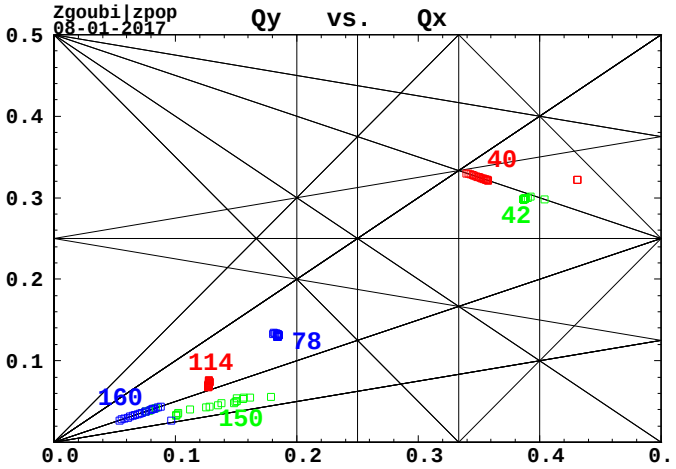

Figure 9: Spreading of $Q_x,\ Q_y$ tunes under the effect of vertical anharmonicities, up to maximum stable vertical amplitude. For each energy a few tune values are plotted, corresponding to particles launched with initial vertical invariants evenly distributed from paraxial to maximum amplitude.

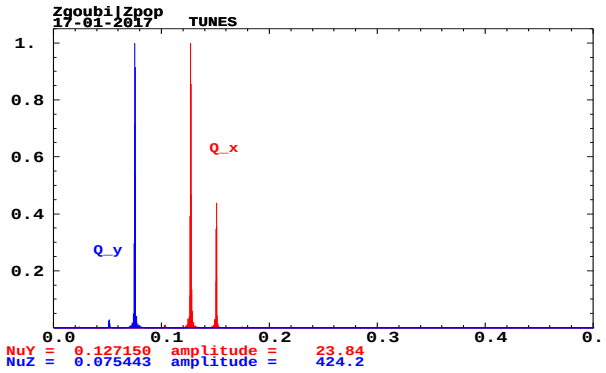

Figure 10: Non-linear motion spectrum at 114 MeV, case of maximum vertical amplitude. Red is H spectrum, blue is V.

Appendix

• Orbit excursions in QF (left) and BD (right), 42, 78, 114 and 150 MeV.

Note that, unlike what is observed here (left plot) the orbits are expected to be centered with respect to QF axis, with about 115∼118 MeV on-axis energy).

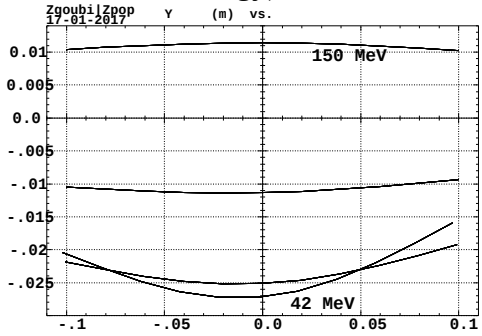

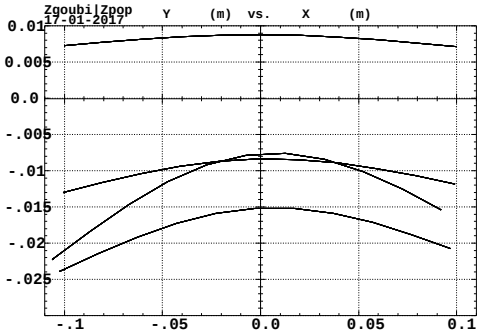

• Vertical field component along orbits in QF (left) and BD (right).

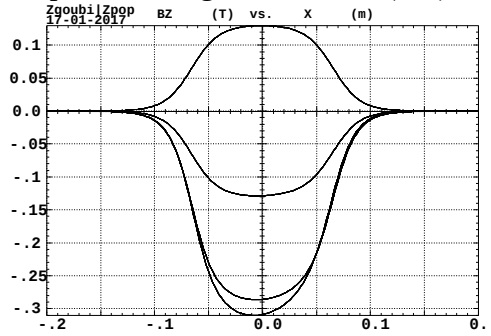

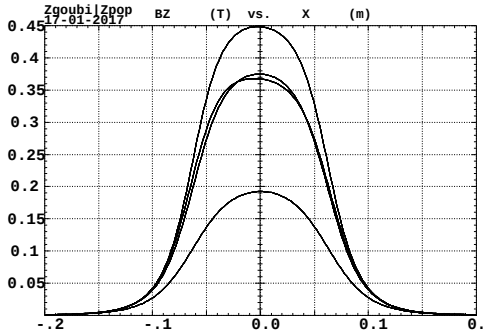

• Zgoubi data file, typical.

```
Data generated by searchCO
'OBJET'
140.086551766     ! 42 MeV total  41.489003 MeV kin
2
4  1
 -1.761206E+00  -1.154222E+02  0. 0. 0.  1.00000000 '1'        41.489003
 -2.037381E+00  -5.824765E+01  0. 0. 0.  1.85724040 '1'        77.489001
 -1.003092E+00  -1.676630E+01  0. 0. 0.  2.71445930 '1'       113.489003
  9.976562E-01   1.640649E+01  0. 0. 0.  3.57167210 '1'       149.489002
 1 1 1 1 1 1 1 1 1 1

 'PARTICUL'
 0.51099892 1.60217653e-19 1.15965218076e-3 0.0 0.0

 'FAISTORE'
 zgoubi.fa
 1

 'DRIFT'  HD2
 6.

 'DRIFT'
 -33.335
 'TOSCA'   QF
 0 0
 -.98e-3 1. 1. 1.
 HEADER_8  ZroBXY
 801 79 31 15.1  1.
 b_QF_v3_x3p9_y1p5_z40.table
 0 0 0 0
 2
 .2
 2  0.   0.  0.
 'DRIFT'
 -33.335

 'DRIFT'    D1
 7.

 'CHANGREF'
 ZR  -2.50000000 YS  0.1035121150

 'DRIFT'
 -34.91468735  ! -33.915
 'TOSCA'   BD
 0  20
 -.98e-3 1. 1. 1.
 HEADER_8  ZroBXY
 801 79 31  15.1  1.0
 b_BD_v3_x3p9_y1p5_z40.table
 0 0 0 0
 2
 .2
 2  0.  0.  0.
 'DRIFT'
 -32.91531265  !-33.915

 'CHANGREF'
 YS  -0.1035121150 ZR  -2.50000000

 'DRIFT'  HD2
 6.


 'FAISCEAU'

 'REBELOTE'
 9   0.2  99
 'END'
```

References

[1] Provided by Nick Tsoupas, BNL C-AD, Dec. 2016.

[2] This is the lessons from the 1950s MURA studies which from the beginning leaned on computer based multi-turn stepwise ray-tracing [5], as well as from recent 150 MeV scaling FFAG ring R/D in Japan [6], and from the EMMA linear FFAG experiment [3] in which the cell happened to be similar to the present one.

[3] S. Machida et al., Acceleration in the linear non-scaling fixed-field alternating-gradient accelerator EMMA, Nature Physics 8, 243247 (2012).

[4] S. Brooks, private communication.

[5] F.T. Cole, O CAMELOT ! A Memoir of the Mura Years, April 1, 1994, Secs. 6.7, 6.8.

[6] And including an FFAG beam line, see for instance : J.B. Lagrange et al., Straight scaling FFAG beam line, NIM A 691 (2012) 5563.